Mechanistic Modeling of the Epoxy−Amine Reaction in the Presence of Polymeric Modifiers by Means of Modulated Temperature DSC

Steven Swier and Bruno Van Mele*

Department of Physical Chemistry and Polymer Science-FYSC (TW), Faculty of Applied Sciences, Vrije Universiteit Brussel-VUB, Pleinlaan 2, B-1050 Brussels, Belgium

Received January 29, 2003; Revised Manuscript Received March 18, 2003

ABSTRACT: A mechanistic kinetic model, based on the reaction of primary and secondary amine functionalities with an epoxy−hydroxyl complex, combined with the occurrence of other equilibrium complexes has been developed by using the complementary information from the nonreversing heat flow and heat capacity from modulated temperature DSC (MTDSC). The model allows for reaction kinetics simulation of the unmodified epoxy−amine systems diglycidyl ether of bisphenol A (DGEBA) + aniline and DGEBA + methylenedianiline (MDA). To simulate the effect of the polymeric modifiers poly(ether sulfone) (PES: $T_g = 223$ °C) and poly(ethylene oxide)-*block*-poly(propylene oxide)-*block*-poly(ethylene oxide) (triblock: $T_g = -70$ °C) on the reaction rate, an additional complex has to be considered between the ether groups of these modifiers and the hydroxyl groups formed. The high interdiffusion rates at the onset of reaction-induced phase separation in the case of the triblock modifier result in a distinct rate increase, which can be predicted on the basis of information about the composition and fraction of the coexisting phases.

1. Introduction

Composite materials based on epoxy resins are widely used for applications where a high modulus, thermal stability and solvent resistance are required. The incorporation of polymeric modifiers that are initially miscible with the epoxy but phase separate during reaction (reaction-induced phase separation or RIPS) has been widely used, for example, to improve the toughness of these materials.[1] The interplay between the rate of phase separation and reaction rate is important for the final morphology and properties of these composites.

The basic steps describing the epoxy−amine reaction are the primary amine−epoxy and secondary amine−epoxy reaction:[2]

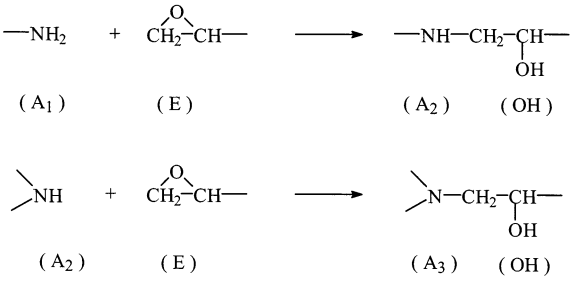

The typical autocatalytic behavior of these systems arises from the formation of a termolecular intermediate with the hydroxyl group formed during the reaction.[3−5] Other complexes arising from hydrogen-bonding interactions render the reaction mechanism more complex.[2] When a certain modifier is added to this low molecular weight epoxy−amine mixture, the dilution of reactive groups is expected to decrease the reaction rate initially. At phase separation, a sudden increase of reaction rate is foreseen due to the concentration increase of reactive groups in the epoxy−amine-rich phase. Rheological changes like gelation and vitrification and effects originating from physical and/or chemical interactions between the modifier and the epoxy−amine can however complicate matters. Moreover, differential segregation of the epoxy and amine components in both phases can occur.[6]

Vitrification interference can be deduced from the position of the cure temperature (T_{cure}) in comparison to (i) the glass transition (T_g) of the homogeneous epoxy−amine/modifier mixture prior to phase separation or (ii) the glass transition of the epoxy−amine-rich phase ($T_{g,\alpha}$) and that of the modifier-rich phase ($T_{g,\beta}$) after RIPS sets in. Knowledge of chemorheological changes in the course of RIPS is crucial as a starting point for a study on the reaction kinetics of modified epoxy thermosets.

Modulated temperature differential scanning calorimetry (MTDSC) is selected in this respect, since it offers benefits for the study of (polymeric) materials, especially when overlapping thermal phenomena occur. A complete discussion of all calculated MTDSC signals can be found in the literature.[7−9] If the phase angle between the heating rate input and the heat flow output signal is considered, in-phase (real) and out-of-phase (imaginary) contributions arise.[9,10] The (modulus of the complex) specific heat capacity, C_p ($J \cdot g^{-1} \cdot K^{-1}$), is calculated as

$$C_p = \frac{A_{HF}}{A_T \omega} \tag{1}$$

where $A_T\omega$ is the amplitude of the imposed modulated heating rate, with A_T the temperature modulation amplitude (K), ω the modulation angular frequency ($=2\pi/p$), and p the modulation period (s); A_{HF} is the amplitude (of the first harmonic) of the resulting modulated heat flow ($W \cdot g^{-1}$). Since the corrected phase

* Corresponding author. E-mail: bvmele@vub.ac.be. Fax: +32-(0)2-629.32.78. Telephone: +32-(0)2-629.32.76 or 32.88.

10.1021/ma034118m CCC: $25.00 © 2003 American Chemical Society
Published on Web 05/16/2003

angle (after corrections for the instrument) is mostly negligible during cure and remains small during vitrification,[11] C_p from eq 1 can be used without corrections for the quantitative interpretation of the results in this paper. The nonreversing heat flow equals the total heat flow (the average of the modulated signal) minus the reversing heat flow (the average heating rate times C_p).

MTDSC is able to measure vitrification effects in the heat capacity signal, while the nonreversing heat flow expresses the reaction exothermicity.[11] This was illustrated for the linearly polymerizing DGEBA + aniline system modified with a high-T_g thermoplastic poly(ether sulfone) (T_g(PES) = 223 °C), where careful selection of T_{cure} resulted in either vitrification of both coexisting phases ($T_{cure} < T_{g,\alpha} < T_{g,\beta}$) or vitrification of only the PES-rich phase ($T_{g,\alpha} < T_{cure} < T_{g,\beta}$).[12] Since the cure of most thermosetting networks has to be performed below their full cure glass transition ($T_{cure} < T_{gfull}$), vitrification of the epoxy−amine-rich phase will occur mostly in the course of RIPS.[12] Depending on $T_{g,\beta}$, vitrification of the modifier-rich phase will also interfere near the onset of RIPS.[12,13] The interdiffusion rates between the coexisting phases change considerably when vitrification of one phase takes place, while phase separation is essentially halted upon vitrification of all phases.[13,14] In the case of the high-T_g modifier PES, a fraction of the epoxy−amine species remains trapped in the modifier-rich phase, and completion of reaction and phase separation can only be attained upon increasing T_{cure} further.[14] Similar effects have been stated for poly(ether imide) (PEI)-modified systems.[13,15] When the low-T_g modifier poly(ethylene oxide)-*block*-poly(propylene oxide)-*block*-poly(ethylene oxide) (triblock: $T_g = -70$ °C) is used, the much higher interdiffusion rates result in clear rate increases at the onset of RIPS due to a concentration rise of reactive groups in the epoxy−amine-rich phase.[13,14] When poly(styrene) (PS: $T_g = 100$ °C) was used instead of PEI ($T_g = 210$ °C) as a modifier for epoxy−amine networks, more pronounced rate increases were also found since the PS-rich phase stays mobile during RIPS at the studied cure temperatures (100 °C < T_{cure} < 210 °C).[16]

Other studies used rheological and dielectrical data to probe vitrification in poly(sulfone) (PSn) and PES-modified network systems.[17−19] Since no simultaneous information on the reaction rate can be obtained with these techniques, no distinction could be made between retardation of the reaction resulting from vitrification and retardation resulting from the dilution of reactive groups. When gelation occurs prior to RIPS, no sudden reaction rate changes were found during cure.[20]

Empirical rate laws expressing the autocatalytic behavior of the epoxy−amine reaction are widely used to determine whether the modifier simply acts as a diluent or interacts (physically or chemically) with the epoxy−amine prior to the onset of phase separation.[16,21−24] Conflicting information is, however, sometimes presented. PEI was found to act as a diluent for the reaction of DGEBA + MCDEA,[16,25] while another work stated an additional catalytic effect of the tertiary nitrogen of PEI for the same epoxy−amine system.[26] In the case of PES and PSn, no physical or chemical interactions with DGEBA and methylenedianiline (MDA) were detected by FT-IR spectroscopy,[17,18] while the hydroxyl end groups of PES have been said to enhance the reaction rate in DGEBA + MCDEA.[25] No interaction was found between poly(methyl methacrylate) (PMMA) and DGEBA using FT-IR and SEC,[20] while a strong interaction exists with the hardener MDA.[27] According to an empirical rate law,[21] this resulted in deviations from the autocatalytic behavior. Also note that preferential interaction of the epoxy or amine component with the modifier can result in differential segregation. Enrichment of the modifier-rich phase in the more compatible epoxy component resulted in an increased reaction rate in the system TGDDM + DDS/PEI[23] and a higher probability of occurrence of side reactions in the system TGAP + DDS/PSn.[24] Chemical reaction between thermoplastics containing functional groups can also occur.[28,29]

Finally, it should be emphasized that the reaction is heterogeneous from the onset of phase separation, resulting in a different conversion advancement in the coexisting phases and a complex morphology development.[30]

While deviations from empirical rate laws can indicate possible physicochemical interactions, a mechanistic approach has the potential of predicting the effect of these interactions on the rate of individual steps in the mechanism. A mechanistic model including both reactive and nonreactive complexes in combination with the amine−epoxy reaction steps has been developed by using the complementary information from MTDSC.[5] While the nonreversing heat flow is proportional to the conversion rate of epoxide groups, the heat capacity is able to distinguish between the primary amine−epoxy and secondary amine−epoxy reaction steps.[31] Solely using the former signal restricts the reaction kinetics model to an empirical approach. The optimized mechanistic model can successfully simulate MTDSC profiles *and* concentration evolutions of reacting species obtained from spectroscopic techniques as a function of time and temperature for different epoxy−amine mixture compositions and for different chemistries.[5,32,33]

This mechanistic approach will be extended for the *modified* epoxy−amine systems by including possible interactions between the modifiers PES and triblock and the epoxy−amines DGEBA + aniline and DGEBA + MDA. The heat capacity signal from MTDSC can be used to define regions in which both phases are mobile (chemically controlled reaction) and regions in which the mobility of either or both phases is restricted (diffusion-controlled reaction). This signal will also be employed together with optical microscopy measurements to detect the onset of phase separation, beyond which the reaction has to be considered in separate phases or thermodynamic open systems.

2. Experimental Section

2.1. Materials. The epoxy resin used in this study is diglycidyl ether of bisphenol A (DGEBA, Epon825 from Shell) with an epoxy equivalent weight (EEW) of 180 g·equiv^{-1}. Reactive mixtures with two amine hardeners were considered: a bifunctional amine (aniline from Fluka) and a tetrafunctional amine hardener (methylenedianiline, MDA from Janssen Chimica) with amine equivalent weights of 46.5 and 49.5 g·equiv^{-1}, respectively. Different mixtures of these pure systems were prepared with different amounts of poly(ether sulfone) (PES, from Aldrich: $M_w = 20\,000$ g mol^{-1}; hydroxy monofunctional; $T_g = 223$ °C) and of the triblock copolymer poly(ethylene oxide)-*block*-poly(propylene oxide)-*block*-poly(ethylene oxide) (triblock; from Aldrich: $M_n = 4400$ g mol^{-1} with 30 wt % ethylene oxide, hydroxy difunctional; $T_g = -70$ °C[13]). A random poly(ethylene oxide)-*co*-poly(propylene oxide) has also been used in a case study (random, from

Aldrich: M_n = 12 000 g mol^{-1} with 75 wt % ethylene oxide; hydroxy difunctional).

To obtain a homogeneous mixture of the high-T_g modified DGEBA + aniline, PES was first dissolved in the epoxy using CH_2Cl_2, which was evaporated at about 120 °C under extensive stirring followed by vacuum evaporation at 100 °C. Aniline was mixed afterward for about 5 min at 80 °C. Because of high mixture viscosity, this method does not allow for the preparation of mixtures with PES contents higher than 30 wt %. Performing the final mixing step at a higher temperature could extend this range, however, at the expense of considerable epoxy−amine reaction. For the network system, the appropriate quantities of all components (DGEBA + MDA/PES) were dissolved in CH_2Cl_2/CH_3OH (99/1), followed by solvent evaporation at 40 and 80 °C under vacuum for 1 h and 5 min, respectively. The DGEBA + MDA/triblock and DGEBA + MDA/random systems were mixed at 80 °C for 5 min. All these preparation methods reduce the amount of preliminary reaction to a minimum.

2.2. Techniques. Cure experiments were performed on a TA Instruments 2920 DSC with MDSC option and a refrigerated cooling system (RCS). Helium was used as a purge gas (25 mL·min^{-1}). Indium and cyclohexane were used for temperature calibration. The former was also used for enthalpy calibration. Heat capacity calibration was performed with a PMMA standard (supplied by Acros)[34] by calibrating the heat capacity *difference* between two temperatures, one above and one below the glass transition temperature of PMMA. In this way, the most accurate and reproducible measurements of heat capacity *changes* were obtained. This is important to adequately detect the reaction heat capacity, $\Delta_r C_p$, attributed to the epoxy−amine reaction.

Cure was performed in hermetic aluminum pans (TA Instruments) with sample weights between 5 and 10 mg. Modulation conditions were as follows: amplitude of 1 °C and a 60 s period. These conditions do not affect the reaction kinetics for the cure temperatures and reactive systems used.[11] Thus, the quasi-isothermal cure condition, arising when a temperature modulation is superimposed on an isothermal temperature program, is an excellent approximation for the strictly isothermal cure.

Cloud points were detected by measuring the light transmitted through thin samples (held between glass slides) in a Mettler Toledo FP82HT hot stage equipped with a photodetector. A Spectratech optical microscope was used with a magnification of 4.

2.3. Optimization Software for Reaction Kinetics Modeling (FITME). The software package FITME enables simulations and kinetic parameter optimizations. FITME is based on OPTKIN, a program for mechanistic modeling using kinetic and thermodynamic parameter optimization.[35] Multiple experiments can be optimized simultaneously with one parameter set. The integration routine uses a fourth-order semiimplicit Runge−Kutta method.[36,37] The optimization routine used[38] is based on a combination of three algorithms for finding the least-squares root: Newton−Raphson, steepest descent, and Marquardt.

3. Results and Discussion

3.1. Reaction Kinetics Model. 3.1.1. Reaction Mechanism for Modified Epoxy—Amines. A reaction mechanism for unmodified epoxy−amine systems was established using a model epoxy−amine phenyl glycidyl ether (PGE) + aniline[5] and was extended to the linearly polymerizing DGEBA + aniline[32] and the network-forming DGEBA + MDA:[33]

Scheme 1

reactive complexes:

$$E + Cat \rightleftharpoons ECat \quad K_{ECat}$$

primary and secondary amine−epoxy reaction:

$$ECat + A_1 \rightarrow OH + A_2 + Cat \quad k_{1Cat}\,(A_{1Cat}, E_{1Cat})$$

$$ECat + A_2 \rightarrow OH + A_3 + Cat \quad k_{2Cat}\,(A_{2Cat}, E_{1Cat})$$

nonreactive complexes:

$$A_1 + OH \rightleftharpoons A_1OH \quad K_{A_1OH}$$

$$Et + OH \rightleftharpoons EtOH \quad K_{EtOH}$$

$$Et + A_1 \rightleftharpoons EtA_1 \quad K_{EtA_1}$$

E is the epoxy, A_1 and A_2 are the primary and secondary amines, respectively, and OH is the hydroxyl group formed during the reaction. Cat designates catalysts OH and A_1; ECat is an equilibrium complex (termed *reactive* complex) that can further react with A_1 or A_2 in the primary and secondary amine−epoxy reaction, respectively. The notation for the equilibrium constant (K) and reaction rate constants (k) with their respective activation energies (E) and preexponential factors (A) are also given. Other *nonreactive* complexes have to be considered between OH and A_1 and the ether group of the epoxy (Et).[2,39] While the reactive complexes (EOH and EA_1) facilitate the reaction causing an accelerated rate, the nonreactive complexes will reduce the concentration of other reactive species and thus retard the reaction.[5]

The polymeric modifiers can result in additional complex formation. In the case of PES and the triblock copolymer, the ether groups in the backbone (termed $Et_{(mod)}$) could interact with the hydroxyl groups formed in the epoxy−amine reaction. Moreover, the modifier can introduce hydroxyl-containing impurities (termed OH_i), which originate from moist or OH end groups, in the reactive mixture:

Scheme 2

$$E + OH_i \rightleftharpoons EOH_i \quad K_{EOH_i}$$

$$EOH_i + A_1 \rightarrow OH + A_2 + OH_i \quad k_{1OH_i}\,(A_{1OH_i}, E_{1OH_i})$$

$$Et_{(mod)} + OH \rightleftharpoons Et_{(mod)}OH \quad K_{Et(mod)OH}$$

Notations are as in Scheme 1.

The reaction of A_2 with the EOH_i complex was found to be negligible in comparison to the reaction with the EOH complex (Scheme 1) due to the high concentration of OH groups at the conversion where the secondary amine−epoxy reaction becomes competitive with the primary amine−epoxy reaction (around 50% conversion[33]). The formation of the equilibrium complexes $Et_{(mod)}A_1$ and A_1OH_i was not included to reduce the number of fitting parameters.

Note that no chemical reactions have been found between PES and DGEBA or MDA,[17,25] while no data are available in this respect for the triblock modifier. In nonisothermal MTDSC experiments on mixtures of DGEBA with PES and DGEBA with the triblock modifier no reaction can be detected below temperatures of 250 and 150 °C, respectively (not shown). The lower end temperature for the triblock copolymer is needed to avoid degradation of this modifier. The onset of degra-

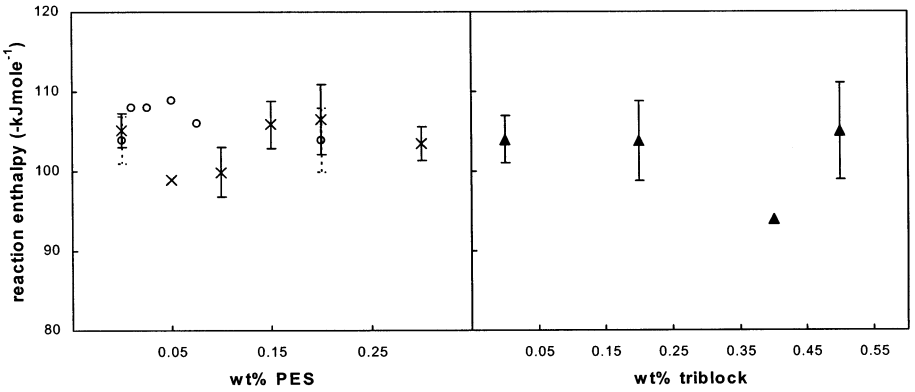

Figure 1. Reaction enthalpy ($\Delta_r H$) normalized per mole of the epoxy group as a function of modifier content for PES-modified, stoichiometric DGEBA + aniline (×) and DGEBA + MDA (○) mixtures and for triblock-modified, stoichiometric DGEBA + MDA mixtures (▲). Error bars are included when more than two measurements were averaged; note that $\Delta_r H$ was obtained both under nonisothermal and under combined isothermal and nonisothermal conditions, in which full cure conditions were ascertained.

dation is greatly postponed when the triblock is present in the (partly) reacted DGEBA + MDA system.

Further confirmation of the absence of chemical reactions between modifier and epoxy−amine can be obtained by analyzing the reaction enthalpy ($\Delta_r H$). Figure 1 depicts $\Delta_r H$ as measured in nonisothermal or combined isothermal and nonisothermal cure schedules. No significant deviations are found in comparison to the unmodified mixtures (0 wt % in Figure 1). This indicates that all reactive epoxy functionalities are consumed by amine groups and do not engage in reactions with the modifier.

The constant $\Delta_r H$ also rules out differential segregation after RIPS sets in. In case preferential diffusion of the epoxy or amine in the modifier-rich phase (termed β phase) would occur, a different mixture composition would be present in each phase. This would leave residual, unreacted groups and thus lower values of $\Delta_r H$.

The glass transition is a very sensitive probe for stoichiometric imbalances.[32,33] Deviations of 5% in the epoxy−amine mixture composition, for example, result in a change of 5 °C in the full cure glass transition of DGEBA + aniline. This notion is exploited here to probe possible deviations in the epoxy−amine ratio in the epoxy−amine-rich phase in the case of the stoichiometric DGEBA + aniline/PES system. It has been shown that the composition of the epoxy−amine-rich phase (termed α phase) of this system is close to pure epoxy−amine for conversions beyond the onset of phase separation.[14] When cure is performed to completion at isothermal cure temperatures above the full cure glass transition of DGEBA + aniline (T_{gfull} = 95 °C), the absence of differential segregation would result in a $T_{g,\alpha}$ close to 95 °C. Mixtures with different modifier contents were cured at temperatures above 95 °C until no more reaction (from the nonreversing heat flow) or phase separation (from the heat capacity) could be detected. The glass transitions of the α phases created in this way are depicted in Figure 2. No significant deviations are found from the case of the unmodified DGEBA + aniline mixture (note error bar for 0 wt % PES).

The constant $\Delta_r H$ and $T_{g,\alpha}$ also indicate that fractionation based on thermodynamics or diffusion,[40] resulting from the polydispersity of the epoxy−amine species, is unlikely.

3.1.2. Experimental Input. The nonreversing heat flow signal ($d_r H/dt$) from MTDSC was found to be

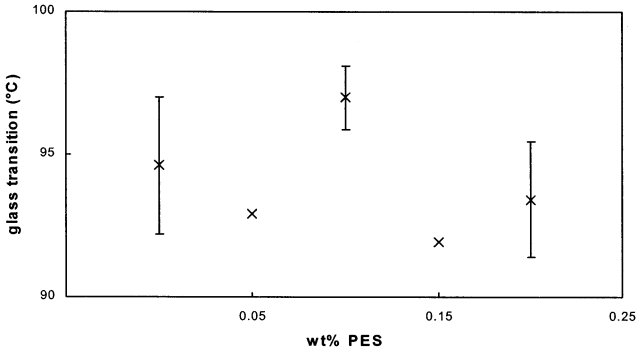

Figure 2. Glass transition of the α phase ($T_{g,\alpha}$) vs the PES content as obtained from isothermal cure experiments above 95 °C and combined isothermal and nonisothermal cure schedules. All cure experiments were averaged (×), and the standard deviation is shown as an error bar.

directly related to the conversion rate of epoxide groups[5,32,33]

$$x(t) = \frac{[\mathrm{E}]_0 - [\mathrm{E}]}{[\mathrm{E}]_0}$$
$$\frac{d_r H}{dt} = \frac{dx}{dt}\Delta_r H \qquad (2)$$

with $[\mathrm{E}]_0$ and [E] the concentration of epoxide groups (in mol·kg^{-1}) at time zero and at time t, respectively, x the epoxy conversion; $\Delta_r H$ is the reaction enthalpy (in kJ·mol^{-1}).

Resolved, mechanistic information is available in the heat capacity signal, since the primary and secondary amine−epoxy reaction steps contribute differently to the reaction heat capacity (in J·mol^{-1}·K^{-1})[31]

$$\Delta_r C_{p,\mathrm{prim}} = a + 0.018(T_{\mathrm{cure}} - 298.15) - 0.00085(T_{\mathrm{cure}} - 298.15)^2$$
$$\Delta_r C_{p,\mathrm{sec}} = b + 0.35(T_{\mathrm{cure}} - 298.15) - 0.00024(T_{\mathrm{cure}} - 298.15)^2 \qquad (3)$$

with $\Delta_r C_{p,\mathrm{prim}}$ and $\Delta_r C_{p,\mathrm{sec}}$ the reaction heat capacities of the primary amine−epoxy and secondary amine−epoxy reaction steps, respectively. a = 18.0 J·mol^{-1}·K^{-1}, b = 19.6 J·mol^{-1}·K^{-1}, and T_{cure} is in K for both DGEBA + aniline[32] and DGEBA + MDA.[33]

Table 1. Optimized Parameters for the Reaction of DGEBA + Aniline and DGEBA + MDA Using the Mechanism of Scheme 1[a]

kinetic parameters ($kg \cdot mol^{-1} \cdot s^{-1}$)						equilibrium constants ($kg \cdot mol^{-1}$)				
k_{1A1}		k_{1OH}		k_{2OH}		K_i				
E_{1A1}	log A_{1A1}	E_{1OH}	log A_{1OH}	E_{2OH}	log A_{2OH}	EOH	A1OH	EA1	EtOH	EtA1
DGEBA + Aniline										
79.6	7.5	48.0	4.4	48.4	4.1	0.20	0.50	0.18	0.55	0.18
DGEBA + MDA										
75.8	7.4	44.0	3.9	48.3	4.2	0.45	0.16	0.18	0.79	0.17

[a] Kinetic (k) and equilibrium (K) parameters are as obtained in refs 32 and 33. Activation energies (E) are in $kJ \cdot mol^{-1}$. Preexponential factors (A) are in $kg \cdot mol^{-1} \cdot s^{-1}$.

Table 2. Optimized Parameters for the Reactions of Modified DGEBA + Aniline and DGEBA + MDA Using the Mechanism Depicted in Schemes 1 and 2[a]

			k_{1OH_i}			
system	[Et(mod)]	$K_{Et(mod)OH}$	E_{1OH_i}	log A_{1OH_i}	$k_{1OH_i}K_{EOH_i}$[b] at 100 °C	[OH_i]
DGEBA + aniline/20 wt % PES	0.9	0.26	52	4.5	3.3	0.05−0.10
DGEBA + MDA/20 wt % PES	0.9	0.40	45	4.1	28	0.07−0.10
DGEBA + MDA/20 wt % triblock	3.7	0.42	45	4.1	28	0.08
DGEBA + MDA/50 wt % triblock	9.3	0.20	45	4.1	28	0.05−0.13
DGEBA + MDA/50 wt % random[c]	10.5	0.50	54	4.2	2.0	0.05

[a] The concentration range of hydroxyl-containing impurities needed to simulate the initial reactivity of the input MTDSC experiments is indicated. The concentrations of ether groups as calculated from the PES and triblock repeat unit are given for each system. All concentrations are in mole per kg total mixture. Activation energy (E) is in $kJ \cdot mol^{-1}$; Preexponential factor (A) is in $kg \cdot mol^{-1} \cdot s^{-1}$. Equilibrium constant ($K$) is in $kg \cdot mol^{-1}$. $k_{1OH_i}K_{EOH_i}$ is in 10^{-4} $kg^2 \cdot mol^{-2} \cdot s^{-1}$. [b] For comparison: $k_{1OH}K_{EOH}$(DGEBA + aniline at 100 °C) = 9.4×10^{-4} $kg^2 \cdot mol^{-2} \cdot s^{-1}$ and $k_{1OH}K_{EOH}$(DGEBA + MDA at 100 °C) = 22×10^{-4} $kg^2 \cdot mol^{-2} \cdot s^{-1}$. [c] A test experiment using a random poly(ethylene oxide)-*co*-poly(propylene oxide) modifier has been optimized also (termed random).

To link $\Delta_r C_{p,prim}$ and $\Delta_r C_{p,sec}$ from eq 3 with the heat capacity changes obtained experimentally with MTDSC, the concentration profiles as calculated in the optimization program will be used

$$\Delta_r C_p = \Delta_r C_{p,prim}([A_2] + [A_3]) + \Delta_r C_{p,sec}[A_3] \quad (4)$$

with [A_i] concentrations in $mol \cdot kg^{-1}$, $\Delta_r C_{p,prim}$ and $\Delta_r C_{p,sec}$ in $J \cdot mol^{-1} \cdot K^{-1}$, and the experimental reaction heat capacity $\Delta_r C_p$ in $J.kg^{-1} \cdot K^{-1}$.

3.1.3. Initial Parameters Set. The rate constants and equilibrium constants needed in Scheme 1 will be fixed to the values found for the unmodified DGEBA + aniline and DGEBA + MDA systems (see Table 1).

Initial parameters for Scheme 2 are taken by considering the reaction steps and equilibrium complexes that are similar to the ones in the unmodified case: $K_{EOH_i} = K_{EOH}$; $K_{Et(mod)OH} = K_{EtOH}$, and $k_{1OH_i} = k_{1OH}$.

To estimate the amount of low molecular weight impurities like water present in PES and the triblock, thermogravimetric analysis was performed on both pure modifiers. A maximum weight loss of 1 wt % was found in a drying procedure at 100 °C. Another source of hydroxyl-containing impurities is the OH end group(s) of these modifiers. Considering these effects and the weight fraction of modifier used, the initial [OH_i] was set in a range from 0.05 to 0.20 $mol \cdot kg^{-1}$. The weight fractions of ether groups ($Et_{(mod)}$) in the modifiers have been calculated from the repeat units of PES and the triblock copolymer (containing 30/70 wt/wt PEO/PPO) at 7 and 30 wt %, respectively.

3.1.4. Optimization. A least sum of squares approach is used to optimize the kinetic model expressed by Schemes 1 and 2. The experimentally obtained nonreversing heat flow and heat capacity from MTDSC are linked to concentration profiles of reactive groups by considering eqs 2 through 4. The optimized parameters are: $K_{Et(mod)OH}$, E_{1OH_i}, and A_{1OH_i}. Since the amount of impurities was difficult to reproduce (see next sections), [OH_i] was varied for each experiment that served as input for the optimization in the range given before. All other parameters were held fixed to values in the initial set.

Isothermal and nonisothermal MTDSC experiments are employed as input for parameter optimization of the following systems: DGEBA + aniline/20 wt % PES; DGEBA + MDA/20 wt % PES; DGEBA + MDA/20 wt % triblock and DGEBA + MDA/50 wt % triblock. Stoichiometric epoxy−amine compositions are used in this work. Optimization of the reaction mechanism was restricted to the region of homogeneous cure by only including conversions until the onset of RIPS as obtained from optical microscopy or heat capacity data.

The optimized set of parameters thus obtained is given in Table 2. Values for $k_{1OH_i}K_{EOH_i}$ and $k_{1OH}K_{EOH}$ (calculated from Table 1) at 100 °C are of the same magnitude. This means that the catalytic activity of the hydroxyl groups present as impurities (OH_i) and those formed in the reaction (OH) are similar. The equilibrium constant of the complex formed between OH and $Et_{(mod)}$ is consistently lower than the one for the complex formed with the ether group of DGEBA (Et). This indicates that the interaction strength of $Et_{(mod)}$ with OH is somewhat lower. Further interpretation of the parameter values in Table 2 will follow in the next sections.

3.2. PES-Modified DGEBA + Aniline. 3.2.1 Isothermal and Nonisothermal Cure of DGEBA + Aniline/20 wt % PES. The effect of cure temperature on the evolution of the nonreversing heat flow and heat capacity signal is depicted in Figure 3 (symbols) for DGEBA + aniline/20 wt % PES.[13] The nonreversing heat flow shows the typical autocatalytic behavior of the epoxy−amine reaction.[41] The initial increase in C_p contains additional mechanistic information about this

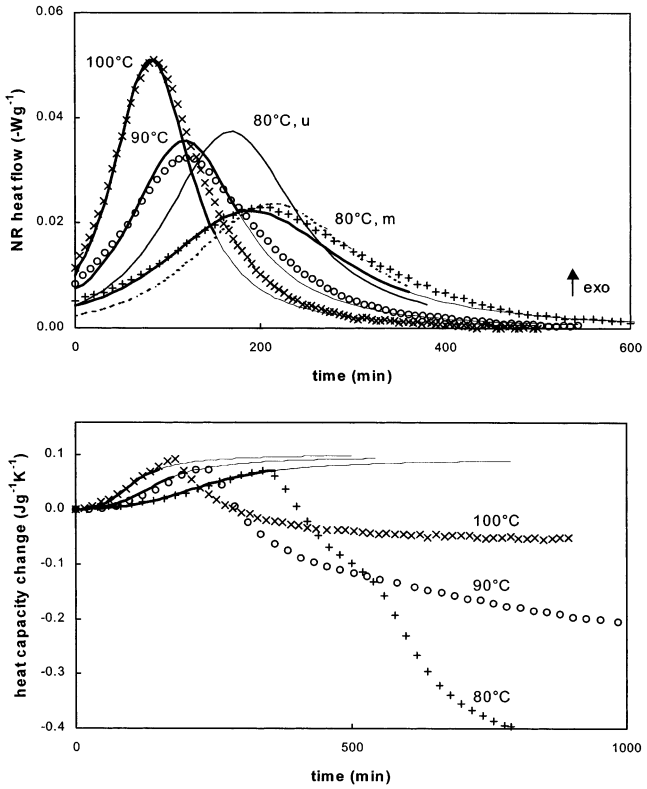

Figure 3. Nonreversing (NR) heat flow and change in heat capacity (note different time scale) from MTDSC for the reactive blend DGEBA + aniline (r = 1)/20 wt % PES cured at 100 (×), 90 (○), and 80 °C (+, modified system m); simulations using the parameter sets of Tables 1 and 2 (thick line until the onset of phase separation, as determined from optical microscopy, and fine line from the onset of phase separation); simulation of the NR heat flow for an unmodified (u) DGEBA + aniline (r = 1) system at 80 °C (parameter set of Table 1) (thin line, u); simulation of the NR heat flow signal by using the parameter set of Table 1 and considering only the dilution of reactive groups is also shown for T_{cure} = 80 °C (dashed line until the onset of phase separation).

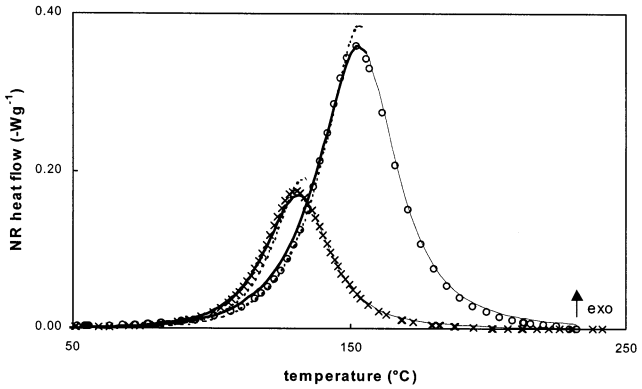

Figure 4. Nonreversing (NR) heat flow for the nonisothermal cure of DGEBA + aniline (r = 1)/20 wt % PES at 1 (×) and 2.5 °C·min^{-1} (○); simulations using the parameter sets of Table 1 and Table 2 (line), where fine line is used from the onset of phase separation as determined from optical microscopy; simulation of the nonreversing heat flow signal by using the parameter set of Table 1 and considering only the dilution of reactive groups (dashed line until the onset of phase separation).

reaction (see eqs 3 and 4 and[31]). The position of T_{cure} in comparison to T_{gfull} (95 °C) determines whether vitrification of only the PES-rich phase (T_{cure} = 100 °C, single stepwise C_p decrease) or both the PES-rich and the epoxy−amine-rich phases occurs (T_{cure} = 90 °C and 80 °C, double stepwise C_p decrease) beyond RIPS, as elaborated upon in ref 13.

The simulation for the reaction at 80 °C of the unmodified DGEBA + aniline system is given for comparison in Figure 3 (thin line). By using the same kinetic and equilibrium parameters from this unmodified case (Table 1) and by assuming only the dilution of reactive groups by the addition of the modifier, a much better prediction can already be obtained (Figure 3, dashed line). This shows the flexibility of the mechanistic approach in respect to the prediction of the effect of additives on the reaction rate.

An even better fit can be obtained, especially in the region below the maximum rate, by including a certain amount of OH impurities (OH_i) and by assuming an interaction between $Et_{(mod)}$ and the OH groups formed during the reaction (thick line in Figure 3).

Simulation of the homogeneous reaction beyond the onset of RIPS (fine line in Figure 3) predicts a smaller reaction rate but does not deviate considerably from the experimental nonreversing heat flow trends. This can be attributed to (i) the restricted interdiffusion rates between the α and β phases due to the proximity of T_{cure} to $T_{g,\alpha}$ and $T_{g,\beta}$, which results in a limited concentration increase of the epoxy−amine species in the α phase[14] and to (ii) the high conversion at which RIPS and vitrification of both phases occur.[13]

A close fit is found for the heat capacity change in the region before RIPS, as also shown in Figure 3. This indicates that the interactions between PES and the epoxy−amine do not introduce major changes in the heat capacity difference between reaction products and reagents.[31]

The simulation capability of the mechanistic approach in a wide T_{cure} range is further confirmed by performing nonisothermal cure experiments (Figure 4). Again, a close fit is found by including the interactions between modifier and OH groups, even in the region where a heterogeneous material is formed by RIPS.

3.2.2. Effect of the PES Content. A changing modifier content is inherently included in the reaction mechanism of Scheme 2 as a dilution of reactive groups and an increase in the concentration of $Et_{(mod)}$ groups. The close fit of the nonreversing heat flow for the isothermal cure at 100 °C using PES contents ranging from 0 to 20 wt % validates this approach (Figure 5).

The three signals obtained from MTDSC are shown in Figure 6 for the isothermal cure at 80 °C with PES contents ranging from 10 to 30 wt %. The poorer agreement of the simulation for the 30 wt % system could be related to experimental problems encountered in preparing mixtures with high PES loadings (see section 2). The general trends, however, are predicted. The stepwise decreases in the heat capacity signal (ΔC_p) accompanied by relaxation peaks in the heat flow phase signal correspond subsequently to vitrification of the β phase and the α phase. The magnitude of ΔC_p and of the relaxation peak reflects the fraction of these phases: higher PES contents result in a larger initial ΔC_p and initial relaxation peak.

Information about the shape of the phase diagram can be obtained by plotting the conversion at the onset of phase separation (x_{ps}) as a function of the modifier content (Δ at T_{cure} = 100 °C in Figure 7). The higher x_{ps} for increasing PES contents indicates that the minimum of the phase diagram lies at least below 10%. The minimum or critical point at low modifier content has

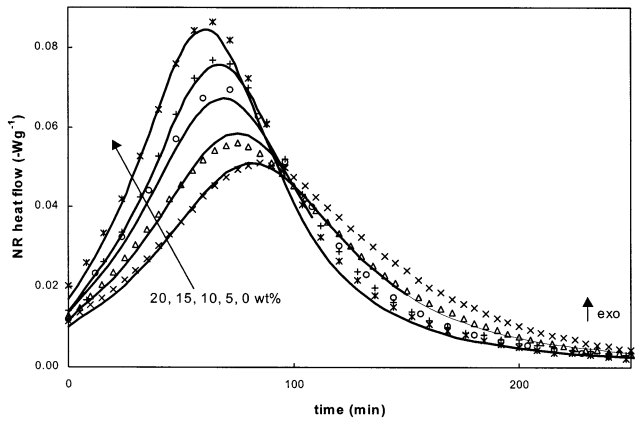

Figure 5. Nonreversing (NR) heat flow for the isothermal cure at 100 °C of DGEBA + aniline ($r = 1$)/PES mixtures with different PES contents: 20 (×), 15 (△), 10 (○), 5 (+) and 0 wt % (∗); simulations using the parameter sets of Tables 1 and 2 (thick line); for 20 wt % PES a fine line is used from the onset of phase separation as determined from optical microscopy (compare × with thin line).

been ascribed to the high molar mass of these thermoplastic modifiers since the critical modifier content is inversely proportional with the square root of the modifier molar mass.[6] Note that the minimum of the phase diagram might not coincide with its critical point due to the polydispersity of both components.[42] The asymmetric shape of the phase diagram of DGEBA + aniline/PES was also concluded from the Temperature-conversion-Transformation TxT diagram constructed for a 20 wt % PES mixture.[13]

Vitrification of the PES-rich phase, which was formed at x_{ps}, occurs when $T_{g,\beta}$ rises above T_{cure}.[14] The conversion at this point ($x_{vitr,\beta}$) is therefore determined by the composition of the β phase. The resulting difference between $x_{vitr,\beta}$ and x_{ps} has been elaborated in detail for the 20 wt % PES mixture.[13,14] Figure 7 includes $x_{vitr,\beta}$ for the isothermal cures at 80 and 100 °C and shows a decreasing trend with PES content. If the coexisting compositions as determined by thermodynamics would be reached instantly, the composition of the β phase at a certain conversion x should be independent of the PES content for a certain T_{cure}. Only the fraction of the β phase would increase with PES content (lever rule).

However, highly restricted interdiffusion rates exist between the α and β phases, especially affecting the composition of the high-T_g β phase.[14] At lower initial PES contents, more interdiffusion has to occur to attain the composition at which $T_{g,\beta}$ equals T_{cure}. This explains the longer cure time or higher $x_{vitr,\beta}$ for lower PES contents in Figure 7.

Although the cloud point for the 30 wt % PES mixture could not be determined with optical microscopy due to the high initial viscosity of the mixture, MTDSC still confirms RIPS for this system at 80 °C (Figure 6). The extrapolation of the x_{ps} line in Figure 7 intersects with the $x_{vitr,\beta}$ line around 30 wt % PES. When T_{cure} is further decreased for the 30 wt % PES system, vitrification of a homogeneous DGEBA + aniline/30 wt % PES mixture might occur. Indeed, isothermal cure at 70 °C for this system results in a single stepwise decrease in ΔC_p and a single relaxation peak in the heat flow phase signal (Figure 8). Note that vitrification of a homogeneous DGEBA + aniline/20 wt % PES mixture was found to occur at 60 °C, although RIPS could still be detected as a double stepwise decrease in ΔC_p in this case.[13]

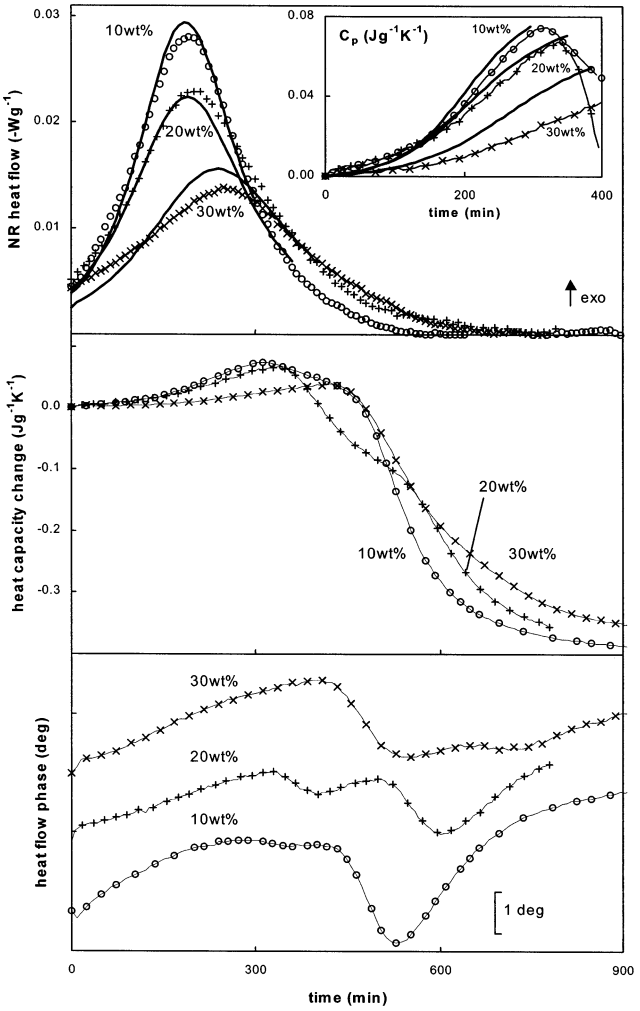

Figure 6. Nonreversing (NR) heat flow, change in heat capacity and heat flow phase from MTDSC for the isothermal cure at 80 °C of DGEBA + aniline ($r = 1$)/PES mixtures with different PES contents: 30 (×), 20 (+), and 10 wt % (○); simulations using the parameter sets of Table 1 and Table 2 (thick line until onset of phase separation as determined from optical microscopy). Data points of the heat capacity and heat flow phase are connected by a fine line for clarity; the inset shows a detail of the reaction heat capacity $\Delta_r C_p$ with the simulation, in the region of a chemically controlled reaction.

3.3. Comparison between PES- and Triblock-Modified DGEBA + MDA. As indicated in Table 2, the concentration of $Et_{(mod)}$ groups introduced in the epoxy−amine mixture by the triblock copolymer is higher than that introduced by the PES modifier. This results in a higher concentration of $Et_{(mod)}OH$ complexes (Scheme 2) for the former system, consequently further decreasing the concentration of OH and thus of EOH complexes. In this way, the autocatalytic behavior of the triblock-modified system will be suppressed to a greater extent. These concepts are illustrated for the DGEBA + MDA system modified with 20 wt % of PES and the triblock in Figure 9. When only dilution of reactive groups is assumed, the rate increase due to autocatalysis is the same for both systems (same amount of modifier) and is overestimated, especially for the low-T_g modifier. The higher reaction rate measured at $t = 0$ results from the presence of hydroxyl-containing impurities OH_i (Table 2). This reaction rate is almost the same or even slightly higher for the PES-modified system, which would not be expected on the basis of its

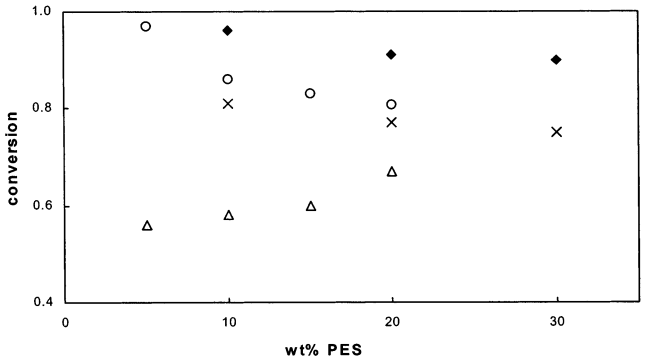

Figure 7. Conversions as a function of the PES content in DGEBA + aniline (r = 1)/PES at: cloud point from optical microscopy (△, T_{cure} = 100 °C); onset of heat flow phase relaxation corresponding to vitrification of β phase (○, T_{cure} = 100 °C and ×, T_{cure} = 80 °C); onset of heat flow phase relaxation corresponding to α phase (◆, T_{cure} = 80 °C). Cloud point could not be determined for the 30 wt % PES mixture due to high initial viscosity.

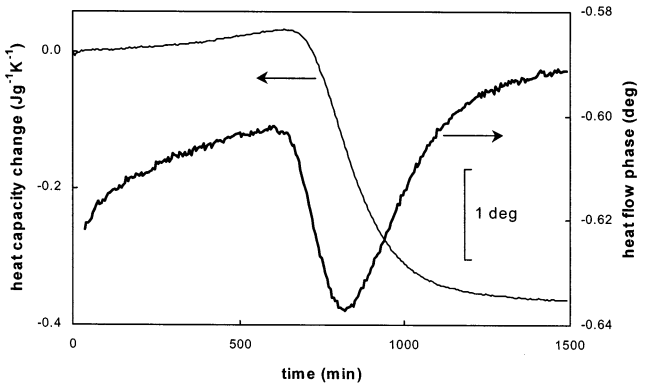

Figure 8. Change in heat capacity and heat flow phase signal from MTDSC for the isothermal cure at 70 °C of a DGEBA + aniline (r = 1)/30 wt % PES mixture.

much higher initial viscosity. The fact that a different viscosity does not affect the reaction rate results from two findings: (i) segment diffusion and not center-of-mass diffusion is important in determining whether chemically controlled or diffusion-controlled reaction takes place,[33] and (ii) T_g of the homogeneous mixture is sufficiently below T_{cure} prior to RIPS.[14]

Note that for the 20 wt % systems in Figure 9, only the difference in $Et_{(mod)}$ concentration is responsible for the changed autocatalytic behavior since $K_{Et(mod)OH}$ is practically the same for both systems (Table 2). The different $K_{Et(mod)OH}$ for the 50 wt % triblock system will be commented upon in the next section.

While simulation and experiment correspond very well for the nonreversing heat flow signal prior to RIPS, the heat capacity signal is less well predicted, especially for the triblock system. This might indicate that corrections are needed to the heat capacity of the products and/or reactants during epoxy−amine cure resulting from specific ether−hydroxyl interactions.[31] The lower $Et_{(mod)}$ concentration for the PES-modified DGEBA + MDA explains the closer fit for this system. Note that both the lower $Et_{(mod)}$ concentration and the smaller $K_{Et(mod)OH}$ probably explain the good $\Delta_r C_p$ prediction for the PES-modified DGEBA + aniline system (see Figure 3 and Table 2).

The simulations, valid for the homogeneous modified systems, have been extended beyond RIPS for comparison (fine line in Figure 9). Note that only chemically controlled reaction has been included in the model of section 3.1. The rate at the final stages of reaction and RIPS due to vitrification of the α phase is therefore overestimated.[33] The accompanying stepwise decrease $\Delta C_{p,vitr}$ is larger for the PES-modified system, corresponding to vitrification of both the β and the α phases. While in the region between the onset of RIPS and prior to vitrification no major deviations are seen in the nonreversing heat flow for the PES-modified system, the triblock-modified system shows an additional peak in this region. This rate increase results from the fast concentration increase of the epoxy−amine species in the α phase, which was initiated at the onset of RIPS.[14] The much smaller interdiffusion rates for the high-T_g modifier, related to the fact that both coexisting phases vitrify, are responsible for the absence of this "concentration effect" in the PES-modified system.

A difference in morphological development should also be considered when comparing the effect of both modifiers on the reaction rate beyond the onset of RIPS. A propylene oxide fraction of 70 wt % in the triblock modifier (see Experimental Section) makes sure that phase separation with epoxy−amines is induced in the micrometer range[43,44] as is the case for the PES-modified systems.[45] When lower propylene oxide fractions or other amphiphilic modifiers are used, nanophase self-assembly results in the formation of nanostructured materials.[44−47] The marked influence of the type and amount of a certain block arises from the fact that the poly(propylene oxide) block becomes immiscible with epoxy−amines at a certain conversion, while the poly(ethylene oxide) block has been stated to be miscible throughout cure.[43,44,48] This results in a complex morphology for the triblock-modified epoxy−amine system as concluded from a peak resolution analysis of the derivative of the heat capacity signal in nonisothermal conditions.[14] Apart from the epoxy−amine-rich phase and the triblock-rich phase, at least two interphases were found in the heterogeneous region. Complex morphologies were also stated consisting of large phases of 30 μm surrounded by interphases with subinclusions on the order of 1 μm.[43]

Another aspect which can greatly influence the phase separation mechanism is the position of the critical point as compared to the used modifier content (20 wt % in this section).[6] Curing a system with modifier contents away from the critical point promotes the nucleation and growth mechanism, while a cure near the critical point composition increases the likeliness of the occurrence of spinodal decomposition. As stated above, the phase diagram of PES-modified systems has an asymmetrical shape with a critical point lying below 20 wt % PES.[13] On the other hand, an analysis of the evolution in composition of the coexisting phases in the triblock-modified system[14] reveals a more symmetrical phase diagram. The effect of these morphological and mechanistic considerations on the observed reaction rate evolution in the heterogeneous region has to be further explored.

3.4. Reaction Rate of DGEBA + MDA Modified with 50 wt % of Low-T_g Copolymers. 3.4.1 Reaction Rate Prior to the Onset of RIPS. The nonreversing heat flow shows an even clearer increase in rate at the onset of RIPS when 50 wt % of the triblock copolymer is added to DGEBA + MDA (symbols in Figure 10). This effect is caused by the higher initial dilution of reactive groups for this mixture together with the fast concen-

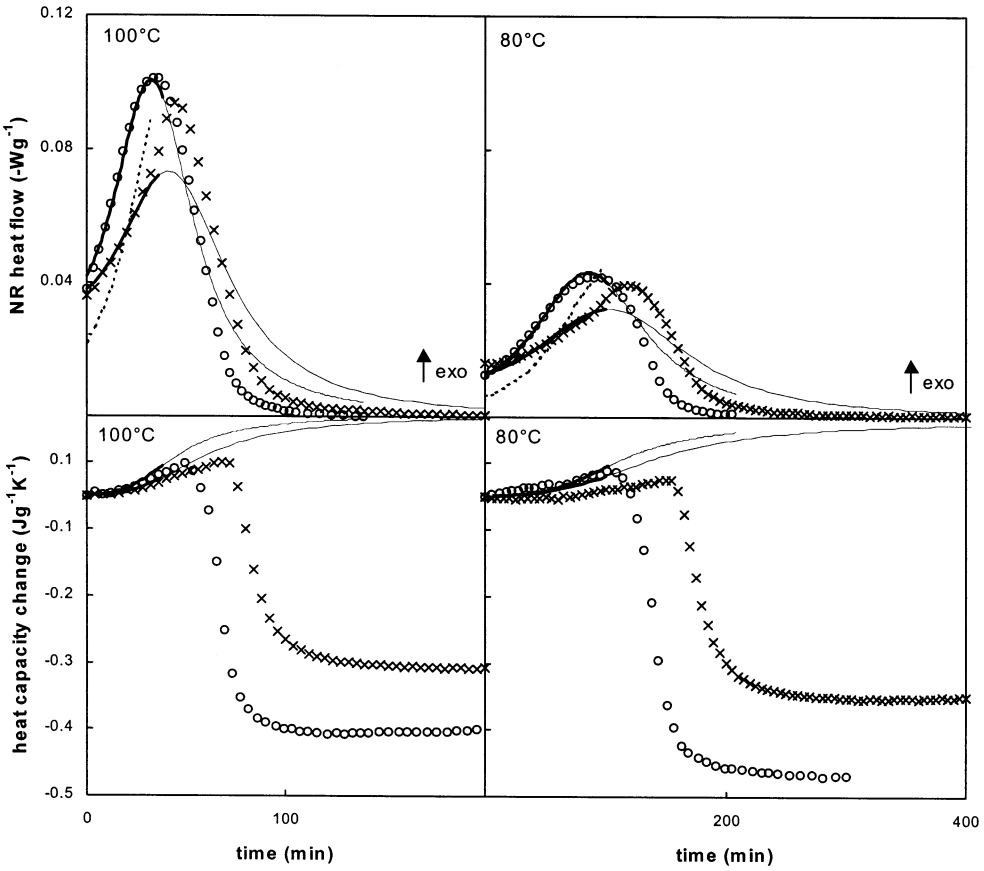

Figure 9. Nonreversing (NR) heat flow and change in heat capacity from MTDSC for the reactive blends DGEBA + MDA (r = 1)/20 wt % PES (○) and DGEBA + MDA (r = 1)/20 wt % triblock (×) cured at 100 (left) and 80 °C (right); simulations using the parameter sets of Tables 1 and 2 (thick line): fine line from the onset of vitrification of the β phase in the case of the PES system (as determined from the relaxation peak in the heat flow phase) and from the onset of phase separation in the case of the triblock system (as determined from optical microscopy); simulation of the NR heat flow signal using the parameter set of Table 1 and considering only the dilution of reactive groups (dashed line until the onset of phase separation).

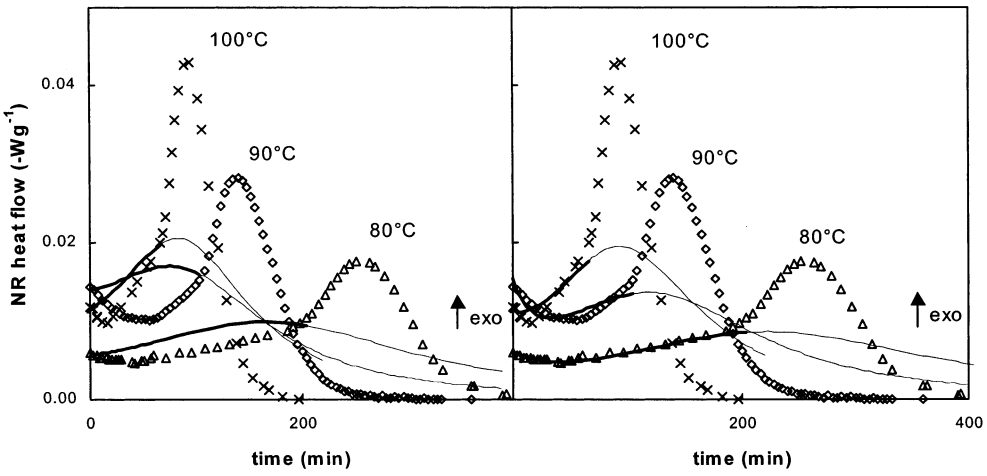

Figure 10. Nonreversing (NR) heat flow for the reactive blend DGEBA + MDA (r = 1)/50 wt % triblock cured at 100 (×), 90 (◇), and 80 °C (△): left side, simulations using the parameter sets of Tables 1 and 2 and Schemes 1 and 2 (line); right side, simulations in which the impurities are assumed to lose their catalytic activity during reaction (see text) (line). A fine line is used from the onset of phase separation as determined from optical microscopy.

tration increase of the epoxy−amine species in the α phase, as explained in the previous section. Moreover, the nonreversing heat flow shows a minimum prior to the onset of RIPS.

This effect cannot be simulated, however, by the optimized model parameters from Schemes 1 and 2 (Table 2). Only the initial reaction rate is predicted in Figure 10 (left side). A better fit can be obtained for the increase in reaction rate after the minimum in the nonreversing heat flow, when a much lower initial reaction rate is assumed (not shown). In this case, the model parameters can merely be considered as fitting parameters with limited physical meaning.

The minimum can be explained qualitatively by considering the high concentration of hydroxyl impurities (OH_i), which results in the prevalence of the

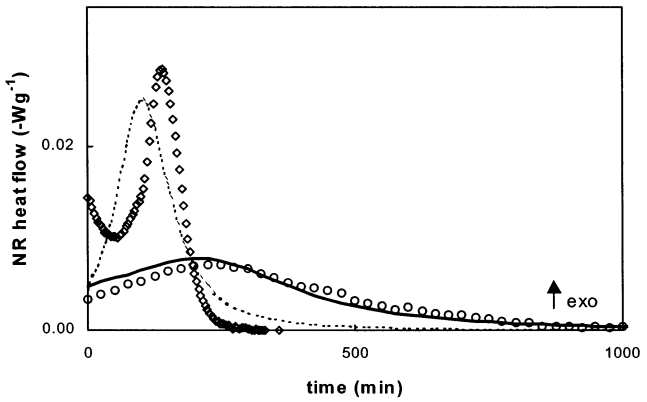

Figure 11. Nonreversing (NR) heat flow for the reactive blend DGEBA + MDA (r = 1)/50 wt % random copolymer cured at 90 °C (○); simulation using the parameter sets of Tables 1 and 2 and Schemes 1 and 2 (thick line); simulation using the parameter set of Table 1 and considering only the dilution of reactive groups (dashed line). The cure at 90 °C for the DGEBA + MDA (r = 1)/50 wt % triblock is repeated for comparison (◇).

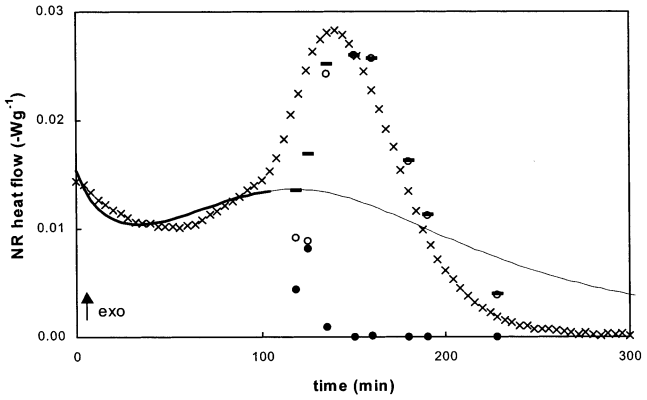

Figure 12. Nonreversing (NR) heat flow for the reactive blend DGEBA + MDA (r = 1)/50 wt % triblock cured at 90 °C (×); simulation of the reaction rate prior to the onset of RIPS (thick line) extrapolation beyond RIPS (fine line); simulation of the reaction rate in the heterogeneous region (−) based on the reaction rate of the epoxy−amine-rich (○) and triblock-rich (●) phases (see text)

primary amine−epoxy reaction catalyzed by OH_i (Scheme 2) in the beginning of the reaction. The initial decrease in reaction rate (e.g.: decrease in the nonreversing heat flow in Figure 10 for the first 50 min at 90 °C) corresponds to the consumption of reactive functionalities (epoxy and amine) in this reaction step. At a certain conversion, the concentration of hydroxyl groups formed during the reaction (OH, Scheme 1) will result in the predominance of the amine−epoxy reaction catalyzed by OH groups, resulting in the measured rate increase (autocatalysis) and explaining the minimum in the nonreversing heat flow signal in Figure 10.

A tentative, alternative explanation is that the hydroxyl impurities lose their catalytic activity during the epoxy−amine cure. The mathematical implementation of this effect in the model consists of using the parameters from Table 2 without modification, while changing the reaction of EOH_i with A_1: $EOH_i + A_1 \rightarrow OH + A_2$ (compare with Scheme 2). In this way, OH_i is "consumed" in this reaction step, and the loss in catalytic activity during reaction is simulated (shown in right side of Figure 10). Note that $K_{Et(mod)OH}$ is lower for this 50 wt % triblock mixture than for the other modified DGEBA + MDA systems in Table 2. The reproducibility of the minimum is, however, poor: the initial reaction rate was found to change up to a factor of 2 for different DGEBA + MDA/50 wt % triblock mixtures. Therefore, no further interpretation of the optimized parameters is attempted. Finally note that the minimum was also found in some mixtures with 20 wt % triblock modifier, although this is not noticeable on the heat flow scale of Figure 9.

As a further indication of the validity of the reaction model in the homogeneous region, a cure experiment on a stoichiometric DGEBA + MDA mixture modified with a random poly(ethylene oxide)-*co*-poly(propylene oxide) modifier (termed random copolymer) is simulated in Figure 11. Because of the much higher PEO content (75 wt %) in this system, no RIPS takes place. The absence of a sudden reactivity increase in this system confirms this statement.

Assuming only the dilution of reactive groups (dashed line in Figure 11) clearly overestimates the reaction rate. By using the parameter sets of Table 1 and Table 2, which include the occurrence of the $Et_{(mod)}OH$ complex, the experimental trend can be simulated until reaction completion. A higher inherent $Et_{(mod)}$ concentration of the random copolymer together with the higher equilibrium constant $K_{Et(mod)OH}$ results in the smaller reactivity of this system in comparison to the triblock system (repeated for comparison in Figure 11).

3.4.2. Reaction Rate beyond the Onset of RIPS. The reaction being monitored beyond the onset of RIPS is a combination of reactions taking place in different phases which are "open thermodynamic systems". These phases should therefore be treated separately in studies of the reaction mechanism. To calculate the reaction kinetics in the heterogeneous region, the concentration of the epoxy−amine species in each phase i as well as the fraction of each phase has to be known. This information was gathered from the derivative of the heat capacity signal (dC_p/dT) in nonisothermal conditions after partial isothermal cure experiments.[14] Using this information, the increase of reaction rate at the onset of phase separation can be predicted (Figure 12). A few assumptions were made to attain this simulation: (i) two separate phases are assumed: an epoxy−amine-rich phase and a triblock-rich phase, (ii) no differential segregation occurs between these phases, and (iii) both phases are assumed to be homogeneous mixtures of the epoxy−amine species and the triblock copolymer for which the reaction rate can be simulated by using Schemes 1 and 2.

The increase in reaction rate of the epoxy−amine-rich phase (○, Figure 12) is clearly responsible for the sudden, global rate increase at phase separation (−, Figure 12). While the simulated reaction rate increase at the onset of RIPS is delayed in comparison to the measured trend, the further evolution of the global reaction rate beyond the onset of RIPS is well predicted and solely related to the rate in the epoxy−amine-rich phase.

Simulations of other cure temperatures require the knowledge of the composition and fraction of the evolving phases as a function of T_{cure} and x. This can be obtained from the dC_p/dT signal as described in ref 14. The procedure to obtain this information is, however, rather time-consuming. A model for the thermodynamics and kinetics of phase separation including the driving force for phase separation and the changing interdiffusion rates, respectively, is therefore of inter-

est.[49] The interplay between these diffusion rates and the reaction kinetics could be established with the mechanistic model providing the conversion x and by using T_g-x relations[32,33] to lay the link with the evolution of molecular weight and cross-link density.

Conclusions

The effect of polymeric modifiers on the reaction rate of epoxy−amine systems can be predicted by including interactions between the modifier and the epoxy−amine species. Chemical reactions do not occur between the epoxy−amines DGEBA + aniline and DGEBA + MDA and the high-T_g modifier PES and the low-T_g triblock copolymer used in this work. The reaction enthalpy, normalized to the epoxy functionality, is constant with modifier content, which confirms that epoxide groups only engage in reactions with amine functionalities and also indicates that differential segregation of the reactive components in the heterogeneous region is unlikely. The glass transition of the epoxy−amine-rich α phase ($T_{g,\alpha}$) is used in the DGEBA + aniline system modified with PES to prove that no deviations from the stoichiometric composition occur, further confirming the previous statements.

Using these findings, a mechanistic model can be presented based on the amine−epoxy reactions and the occurrence of reactive and nonreactive transition complexes. A complex between the ether groups of the modifiers and the hydroxyl groups formed during the epoxy−amine reaction models the physical interaction between modifier and epoxy−amine species. Hydroxyl-containing impurities in the modifiers, arising from moist or OH end groups, are needed to correctly describe the initial reaction rate of these systems. The reaction rate in the homogeneous region prior to the onset of RIPS can be simulated adequately for different modified epoxy−amine systems with this model.

The effect of PES and its content on reactivity, as experimentally obtained from the nonreversing heat flow and heat capacity from MTDSC, can be simulated in this way for the DGEBA + aniline/PES system. Moreover, information about the shape of the phase diagram can be obtained from the conversion at phase separation (optical microscopy) and the conversion at vitrification of the PES-rich β phase (heat capacity signal) as a function of PES content. The positive slope of the former evolution confirms that the critical point lies at least below 10% for this high molecular weight modifier, while the negative slope of the latter indicates the restricted interdiffusion rates for PES-modified epoxy−amine systems.

The reaction rate in the heterogeneous region can still be predicted using the homogeneous reaction model for the DGEBA + aniline/PES system due to the proximity of T_{cure} to $T_{g,\alpha}$ and $T_{g,\beta}$. This also holds for the PES-modified network-forming DGEBA + MDA system, although the lower conversion at vitrification of the α phase results in an overestimation of the reaction rate in the final stages of reaction. The much higher interdiffusion rates arising at the onset of RIPS for the triblock-modified DGEBA + MDA system result in a clear reactivity increase for this system, especially when a higher triblock content is used. In contrast, the autocatalytic behavior is less distinct in comparison to the PES-modified systems since a higher ether concentration in the triblock copolymer decreases the concentration of EOH complexes to a greater extent. Further research has to elucidate whether the difference in phase separation mechanism and/or morphological evolution for both polymeric modifiers has an additional contribution to the reaction rate difference in the heterogeneous region.

The reactivity increase accompanying RIPS in the triblock system has been predicted on the basis of the evolution of the composition and fraction of the coexisting phases obtained from dC_p/dT data. By considering an epoxy−amine-rich and triblock-rich phase and by using the homogeneous reaction model in both phases, the experimentally obtained increase of reaction rate at the onset of RIPS and its further evolution can be predicted. To simulate the composition and fraction of coexisting phases, a phase separation model based on thermodynamic and kinetic considerations is required. The interplay between phase separation and reaction could be included by considering the relation between the epoxy conversion and the evolving molecular weight and cross-link density of the epoxy−amine species.

Acknowledgment. The work of S.S. was supported by grants of the Flemish Institute for the Promotion of Scientific-Technological Research in Industry (I.W.T.).

References and Notes

(1) Bucknall, C. B.; Partridge, I. K. *Polymer* **1983**, *24*, 639.
(2) Rozenberg, B. A. *Adv. Polym. Sci.* **1986**, *75*, 113.
(3) Shechter, L.; Wynstra, J.; Kurkjy, R. P. *Ind. Eng. Chem.* **1956**, *48*, 94.
(4) Smith, I. R. *Polymer* **1961**, *2*, 95.
(5) Swier, S.; Van Mele, B. *Thermochim. Acta*, submitted.
(6) Williams, R. J. J.; Rozenberg, B. A.; Pascault, J.-P. *Adv. Polym. Sci.* **1997**, *95*, 128.
(7) Reading, M.; Luget, A.; Wilson, R. *Thermochim. Acta* **1994**, *238*, 295.
(8) Wunderlich, B.; Jin, Y.; Boller, A. *Thermochim. Acta* **1994**, *238*, 277.
(9) Reading, M. *Trends Polym. Sci.* **1993**, *8*, 248.
(10) Schawe, J. E. K. *Thermochim. Acta* **1995**, *261*, 183; *Thermochim. Acta* **1997**, *304/305*, 111.
(11) Van Assche, G.; Van Hemelrijck, A.; Rahier, H.; Van Mele, B. *Thermochim. Acta* **1997**, *304/305*, 317.
(12) Swier, S.; Van Mele, B. *Thermochim. Acta* **1999**, *330*, 175.
(13) Swier, S.; Van Mele, B. *Polymer* **2003**, *44*, 2689.
(14) Swier, S.; Van Mele, B. *Polymer*, submitted for publication.
(15) Barral, L.; Cano, J.; Lopez, J.; Lopez-Bueno, I.; Nogueira, P.; Torres, A.; Ramirez, C.; Abad, M. J. *Thermochim. Acta* **2000**, *344*, 127.
(16) Bonnet, A.; Pascault, J. P.; Sautereau, H.; Taha, M. *Macromolecules* **1999**, *32*, 8517.
(17) Martinez, I.; Martin, M. D.; Eceiza, A.; Oyanguren, P.; Mondragon, I. *Polymer* **2000**, *41*, 1027.
(18) MacKinnon, A. J.; Jenkins, S. D.; McGrail, P. T.; Pethrick, R. A. *Macromolecules* **1992**, *25*, 3492.
(19) Alig, I.; Jenninger, W.; Junker, M.; de Graaf, L. A. *J. Macromol. Sci.: Phys.* **1996**, *B35*, 563.
(20) Ritzenthaler, S.; Girard-Reydet, E.; Pascault, J. P. *Polymer* **2000**, *41*, 6375.
(21) Remiro, P. M.; Riccardi, C. C.; Corcuera, M. A.; Mondragon, I. *J. Appl. Polym. Sci.* **1999**, *74*, 772.
(22) Fernandez, B.; Corcuera, M. A.; Marieta, C.; Mondragon, I. *Eur. Polym. J.* **2001**, *37*, 1863.
(23) Su, C. C.; Woo, E. M. *Polymer* **1995**, *36*, 2883.
(24) Varley, R. J.; Hodgkin, J. H.; Hawthorne, D. G.; Simon, G. P.; McCulloch, D. *Polymer* **2000**, *41*, 3425.
(25) Bonnaud, L.; Pascault, J. P.; Sautereau, H. *Eur. Polym. J.* **2000**, *36*, 1313.
(26) Girard-Reydet, E.; Riccardi, C. C.; Sautereau, H.; Pascault, J. P. *Macromolecules* **1995**, *28*, 7608.
(27) Mondragon, I.; Remiro, P. M.; Martin, M. D.; Valea, A.; Franco, M, Bellenguer, V. *Polym. Int.* **1998**, *47*, 152.
(28) Hseih, H. K.; Su, C. C.; Woo, E. M. *Polymer* **1998**, *39*, 2175.
(29) Hourston, D. J.; Schafer, F.-U. *High Perform. Polym.* **1996**, *8*, 19.

(30) Tran-Cong, Q.; Shibayama, M. In *Structure and Properties of Multiphase Polymeric Materials*; Araki, T., Ed.; Marcel Dekker: New York, 1998.
(31) Swier, S.; Van Mele, B. *J. Polym. Sci.: Part B* **2003**, *41*, 595.
(32) Swier, S.; Van Mele, B. *J. Appl. Polym. Sci.*, in press.
(33) Swier, S.; Van Assche, G.; Van Mele, B. *J. Appl. Polym. Sci.*, in press.
(34) Gaur, U.; Wunderlich, B. *J. Phys. Chem. Ref. Data* **1982**, *11*, 313.
(35) Huybrechts, G.; Van Assche, G. *Comput. Chem.* **1998**, *22*, 413.
(36) Turányi, T. *Comput. Chem.* **1990**, *14*, 253.
(37) Gottwald, B. A.; Wanner, G. *Simulation* **1982**, *37*, 169.
(38) VA05, Harwell Subroutine Library, Release 11; AEA Technology: Harwell, England, 1993.
(39) Enikolopiyan, N. S. *Pure Appl. Chem.* **1976**, *48*, 317.
(40) Borrajo, J.; Riccardi, C. C.; Williams, R. J. J.; Cao, Z. Q.; Pascault, J. P. *Polymer* **1995**, *36*, 3541.
(41) Barton, J. M. *Adv. Polym. Sci.* **1985**, *72*, 111.
(42) Ellianidis, S.; Higgins, J. S.; Clarke, N.; McLeish, C. B.; Choudhery, R. A.; Jenkins, S. D. *Polymer* **1997**, *38*, 4855.
(43) Mijovic, J.; Shen, M.; Wing, Sy J. *Macromolecules* **2000**, *33*, 5235.
(44) Guo, Q.; Thomann, R.; Gronski, W.; Thurn-Albrecht, T. *Macromolecules* **2002**, *35*, 3133.
(45) Inoue, T. *Prog. Polym. Sci.* **1995**, *20*, 119.
(46) Hillmyer, M. A.; Lipic, P. M.; Hadjduk, D. A.; Almdal, K.; Bates F. S. *J. Am. Chem. Soc.* **1997**, *119*, 2749.
(47) Lipic, P. M.; Bates, F. S.; Hillmyer, M. A. *J. Am. Chem. Soc.* **1998**, *120*, 8963.
(48) Zheng, S.; Zhang, N.; Luo, X.; Ma, D. *Polymer* **1995**, *36*, 3609.
(49) Chan, P. K, Rey, A. D. *Macromolecules* **1997**, *30*, 2135.

MA034118M